ISSN 1674-1056
http://cpb.iphy.ac.cn
http://iopscience.iop.org/cpb
中国物理 B
Chinese Physics
中国物理 Chinese Physics B

Quantitative evaluation of space charge effects of laser-cooled three-dimensional ion system on a secular motion period scale

Li-Jun Du(杜丽军), Hong-Fang Song(宋红芳), Shao-Long Chen(陈邵龙), Yao Huang(黄垚), Xin Tong(童昕), Hua Guan(管桦), Ke-Lin Gao(高克林)
Citation: Chin. Phys. B . 2018, 27(4): 043701. **doi:** 10.1088/1674-1056/27/4/043701

Journal homepage: http://cpb.iphy.ac.cn; http://iopscience.iop.org/cpb

What follows is a list of articles you may be interested in

Quantitative evaluation of space charge effects of laser-cooled three-dimensional ion system on a secular motion period scale

Li-Jun Du(杜丽军), Hong-Fang Song(宋红芳), Shao-Long Chen(陈邵龙), Yao Huang(黄垚), Xin Tong(童昕), Hua Guan(管桦), Ke-Lin Gao(高克林)
Chin. Phys. B . 2018, 27(4): 043701. **doi:** 10.1088/1674-1056/27/4/043701

An optimized ion trap geometry to measure quadrupole shifts of ^{171}Yb+ clocks

N Batra, B K Sahoo, S De
Chin. Phys. B . 2016, 25(11): 113703. **doi:** 10.1088/1674-1056/25/11/113703

Determination of ion quantity by using low-temperature ion density theory and molecular dynamics simulation

Du Li-Jun, Song Hong-Fang, Li Hai-Xia, Chen Shao-Long, Chen Ting, Sun Huan-Yao, Huang Yao, Tong Xin, Guan Hua, Gao Ke-Lin
Chin. Phys. B . 2015, 24(11): 113703. **doi:** 10.1088/1674-1056/24/11/113703

Compensating for excess micromotion of ion crystals

Du Li-Jun, Chen Ting, Song Hong-Fang, Chen Shao-Long, Li Hai-Xia, Huang Yao, Tong Xin, Guan Hua, Gao Ke-Lin
Chin. Phys. B . 2015, 24(8): 083702. **doi:** 10.1088/1674-1056/24/8/083702

Implementation of ternary Shor's algorithm based on vibrational states of an ion in anharmonic potential

Liu Wei, Chen Shu-Ming, Zhang Jian, Wu Chun-Wang, Wu Wei, Chen Ping-Xing
Chin. Phys. B . 2015, 24(3): 033701. **doi:** 10.1088/1674-1056/24/3/033701

Quantitative evaluation of space charge effects of laser-cooled three-dimensional ion system on a secular motion period scale*

Li-Jun Du(杜丽军)[1,2], Hong-Fang Song(宋红芳)[2,3,4,5], Shao-Long Chen(陈邵龙)[2,3,4,5], Yao Huang(黄垚)[2,3,4], Xin Tong(童昕)[2,3,4], Hua Guan(管桦)[2,3,4,†], and Ke-Lin Gao(高克林)[2,3,4]

[1] China Academy of Space Technology (Xi'an), Xi'an 710100, China
[2] State Key Laboratory of Magnetic Resonance and Atomic and Molecular Physics, Wuhan Institute of Physics and Mathematics, Chinese Academy of Sciences, Wuhan 430071, China
[3] Key Laboratory of Atomic Frequency Standards, Wuhan Institute of Physics and Mathematics, Chinese Academy of Sciences, Wuhan 430071, China
[4] Center for Cold Atom Physics, Chinese Academy of Sciences, Wuhan 430071, China
[5] University of Chinese Academy of Sciences, Beijing 100049, China

(Received 3 November 2017; revised manuscript received 21 December 2017; published online 10 March 2018)

In this paper, we introduce a method of quantitatively evaluating and controlling the space charge effect of a laser-cooled three-dimensional (3D) ion system in a linear Paul trap. The relationship among cooling efficiency, ion quantity, and trapping strength is analyzed quantitatively, and the dynamic space distribution and temporal evolution of the 3D ion system on a secular motion period time scale in the cooling process are obtained. The ion number influences the eigen-micromotion feature of the ion system. When trapping parameter q is ~ 0.3, relatively ideal cooling efficiency and equilibrium temperature can be obtained. The decrease of axial electrostatic potential is helpful in reducing the micromotion heating effect and the degradation in the total energy. Within a single secular motion period under different cooling conditions, ions transform from the cloud state (each ion disperses throughout the envelope of the ion system) to the liquid state (each ion is concentrated at a specific location in the ion system) and then to the crystal state (each ion is subjected to a fixed motion track). These results are conducive to long-term storage and precise control, motion effect suppression, high-efficiency cooling, and increasing the precision of spectroscopy for a 3D ion system.

Keywords: space charge effects, cooling dynamics, ion trajectory, ion energy

PACS: 37.10.Ty, 37.10.Rs, 37.90.+j, 31.15.xv **DOI:** 10.1088/1674-1056/27/4/043701

1. Introduction

The laser cooling process of a 3D ion system is primarily affected by radio frequency (RF), axial electrostatic potential trapping force, laser cooling force (when a cooling laser is red-detuned), Coulomb interaction among ions, residual gas in a vacuum background, and other random interaction forces between ions and the environment in a linear Paul trap. The kinetic equation for a specific ion in the ion system can be expressed as

$$\begin{aligned} M_i \frac{\mathrm{d}\boldsymbol{r}^2}{\mathrm{d}^2 t} &= F_i(\boldsymbol{r}_1,\ldots,\boldsymbol{r}_N,\boldsymbol{v}_1,\ldots,\boldsymbol{v}_N,t) \\ &= \boldsymbol{F}_i^{\mathrm{trap}} + \boldsymbol{F}_i^{\mathrm{Coulomb}} + \boldsymbol{F}_i^{\mathrm{random}} + \boldsymbol{F}_i^{\mathrm{laser}}, \end{aligned} \tag{1}$$

where $i = 1,\ldots,N-1, N$, with N being the ion ordinal number; M_i, $\boldsymbol{r}_i$, and $\boldsymbol{v}_i$ denote the mass, position vector, and velocity vector of the i-th ion, respectively.

The i-th ion experiences Coulomb interaction force from all other ions, which can be expressed as follows:

$$\boldsymbol{F}_i^{\mathrm{Coulomb}} = \frac{Q_i}{4\pi\varepsilon_0}\nabla \sum_{j=1,j\neq i}^{j=N} \frac{Q_j \boldsymbol{r}_{ij}}{r_{ij}}, \tag{2}$$

where r_{ij} is the distance between the i-th and j-th ions, $\boldsymbol{r}_{ij}$ is a unit vector, and ε_0 is the vacuum permittivity. This is the process of N-body long-range interaction and a physical source of the space charge effect.[1] The detailed analyses of the rest of the forces in the kinetic processes of trapping and cooling in an ion system are shown in Ref. [2]. The range of the Coulomb interaction force among multiple ions is the Debye length, $\lambda_{\mathrm{D}} = (k_{\mathrm{B}}T\varepsilon_0/nQ^2)^{1/2}$,[3] in a linear Paul trap. When this length is less than the spatial extent of the ion system, the space charge effect is the primary interaction in the ion system. As a result, the equivalent harmonic pseudopotential, spatial distribution, harmonic frequency, cooling efficiency, heating efficiency, equilibrium energy, quantum coherence property, and other characteristics of the ion system change to different extents.[4,5] Thus, the systematic evaluation and precise control of the space charge effect are considerably important for realizing the measurement for approximating the theoretical

*Project supported by the National Key Research and Development Program of China (Grant No. 2017YFA0304401), the National Natural Science Foundation of China (Grant Nos. 11622434, 11474318, 91336211, and 11634013), the Strategic Priority Research Program of the Chinese Academy of Sciences (Grant No. XDB21030100), Hubei Province Science Fund for Distinguished Young Scholars (Grant No. 2017CFA040), and the Youth Innovation Promotion Association of the Chinese Academy of Sciences (Grant No. 2015274).

†Corresponding author. E-mail: guanhua@wipm.ac.cn

© 2018 Chinese Physical Society and IOP Publishing Ltd

precision limit in a 3D ion system.

The motion of the 3D ion system in a linear Paul trap includes secular motion and micromotion.[6] The energy, temperature, and other properties of ions can be quantitatively evaluated based on secular motion and micromotion. The sum of the kinetic energies of the two motions is referred to as the total energy of the ions, and the corresponding temperature is referred to as the total temperature[7,8] of the ions. There is a correlation effect between the micromotion and secular motion of the ion system, and the micromotion energy of a cold ion system is typically transferred to the secular motion[9] of the ion system through random interactions between ions and between ions and the environment. The secular energy of ions increases continuously for the irreversibility of random interactions. The space charge effect results in the space distribution of the 3D ion system beyond the nodal line of a radial RF field. There is approximately isotropic Coulomb force coupling between ions, and there is a difference in magnitude of micromotion intensity between the inner ions and the outer ions. The strong micromotion energy of the outer ions is partly coupled into the secular motion of ions in the form of chaotic heating, and the mechanism of RF micromotion heating becomes the most significant obstacle in realizing the efficient cooling and ultralow equilibrium temperature of the 3D ion system. Quantitatively studying the dominant physical parameters of the space charge effect, evaluating their influences on the dynamic characteristics of ion cooling, and exploring a method of precisely regulating and suppressing the space charge effect are the keys to realizing the long-term trapping and precision control of an ultracold 3D ion system.

In this paper, we present a method of quantitatively estimating the space charge effect of the ion system. The method is based on molecular dynamics simulation. First, we quantitatively evaluate the influences of the space charge effect on cooling efficiency and equilibrium temperature for different ion quantities, RFs, and electrostatic trapping fields. Then, the dynamic space distribution and temporal evolution of the 3D ion system on a secular motion period scale are analyzed precisely in different energy states of the cooling process. Finally, the control method and parameter matching for the space charge effect of the 3D ion system are discussed.

2. Experimental setup

The linear Paul trap and the corresponding coordinates used in the experiment are shown in Fig. 1. A detailed description of the experimental setup can be found in Ref. [10]. The lengths of the trapping part (B) and the remaining parts (A, C) of each electrode are $2z_0 = 5.90$ mm and $2z_e = 24.00$ mm, respectively. The diameter of each electrode rod is $d = 8.00$ mm, and the minimum distances between the trap centerline and electrodes are all $r_0 = 3.50$ mm. The confinement of the ions in the radial plane is obtained by applying a pair of RF fields $(\pm(1/2)U_{\rm rf}\cos(\Omega_{\rm rf}t))$ with the same frequency and amplitude and π phase difference to two pairs of diagonal electrode rods ($A_{1,3}$, $B_{1,3}$, $C_{1,3}$, and $A_{2,4}$, $B_{2,4}$, $C_{2,4}$). The RF is 3.80 MHz, and the RF amplitude, $(1/2)U_{\rm rf}$, can be adjusted from 40 V to 200 V. The confinement of the ions in the axial direction is obtained by applying direct current voltage to the end parts of electrodes A and C in a range of 0.010 V–20.000 V. The $^{40}Ca^{+}$ ions ($m_i = 40$ a.u.) are trapped in the linear trap, and the ion simulation parameters are selected based on experiments.

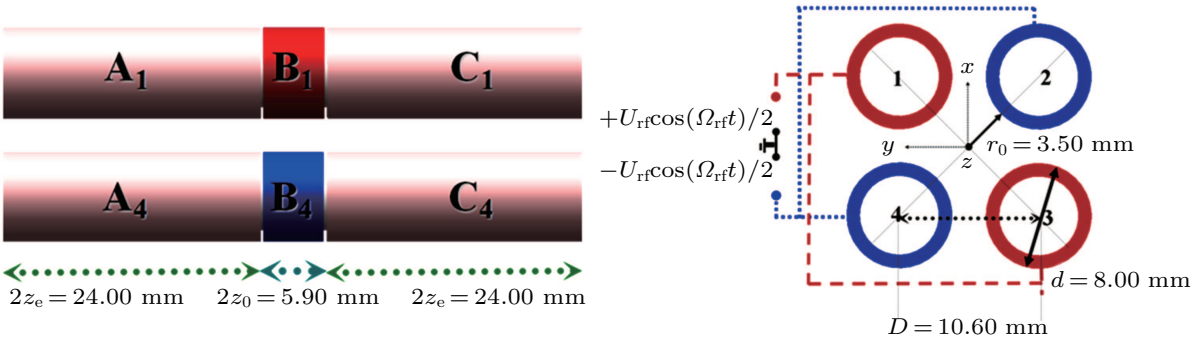


Fig. 1. (color online) Sketch of the linear Paul trap and RF potential.

In order to quantitatively describe the dynamic temporal evolution, the ion dynamic temporal process will be split into equal time intervals in the numerical calculation, and the dynamic equations will be established and solved for all ions at any moment. The time interval of the adjacent moment is called the time step Δt of the numerical calculation. When we solve the equations of position and velocity vectors at the next moment, the position and velocity vectors at the present moment and those at the last moment are used as initial values, and a Taylor expansion with four-order accuracy should be adopted in the approximation. In this process, half of a time step $(1/2)\Delta t$ is the time interval, and the position and velocity vectors of all ions are calculated alternately at all moments. In this calculation process, the position and velocity vectors of all ions will be calculated alternately with a $(1/2)\Delta t$ time interval, analogous to two alternately leaping frogs. There-

fore, this numerical calculation is called the "Leap Frog" algorithm. The "leap frog" algorithm[11–13] is used to solve the equation of motion of the i-th ion. The calculation time step, Δt, is selected to be 1/30 of an RF period. To determine the kinematic and dynamic characteristics of the ion cooling process, the simulation is performed in the following manner: the initial temperature of the ion cloud is set to be 400 K. The kinematics information is monitored while the cloud is moving under the influence of the RF trapping field, Coulomb interaction forces, random collision force, and laser light interaction force. A typical evolution time is 10^5–10^7 RF oscillation periods.

3. Space charge effect of ions in cooling process

The space charge effect is a dynamic spatial distribution effect of ions, dominated by the long-range Coulomb interaction between multiple ions. It varies significantly with ion number and the parameters of the trapping field. The cooling characteristics of ions under different ion numbers and trapping field parameters are examined in detail to systematically analyze the influence of the space charge effect on the cooling dynamic characteristics of the 3D ion system. The dynamic space distribution and temporal evolution characteristics of the 3D ion system in the cooling process are studied quantitatively. In our linear Paul trap, one $^{40}Ca^+$ ion to a few thousand $^{40}Ca^+$ ions can be trapped steadily. We select the number of $^{40}Ca^+$ ions as 320, which can represent the characteristics of the 3D ion system and is not too complicated for calculation.

3.1. Influences of number of trapped ions on cooling efficiency and equilibrium temperature of ions

Tens of millions of ions can be trapped steadily in a linear Paul trap.[14] When a single ion is trapped, it remains close to the nodal line of pseudopotential, obeying a simple motion law that can be described by the harmonic oscillator model. When a few ions are trapped, they are located along the axis of the liner Paul trap in a chain-like manner, and the interaction between the ions is primarily in the axial direction. When a large number of ions are trapped, the ion system is distributed in three dimensions, and the model of harmonic pseudopotential must be corrected by considering the influence of the space charge effect. Different ion numbers result in different space distributions, interaction methods and intensities, and cooling factors of the ion system. This affects the cooling efficiency and equilibrium temperature characteristics of the ion system.

Figure 2 shows the temporal evolution characteristics of the secular and total energies of a single ion and the 3D ion system in the cooling process, with the same experimental parameters and the same initial secular temperature of 400 K. In the cooling process, the evolution trend of the secular energy of a single ion is similar to that of the total energy. When the ion is cooled to the equilibrium state, it remains at the nodal line of harmonic pseudopotential, the heating rate is extremely low, the secular and total temperatures can reach as low as a few milliKelvins, and the stochastic force in the environment is a leading factor that restricts the further decrease in the equilibrium secular temperature of the ion to the Doppler cooling limit. For the 3D ion system, the space charge effect leads to the space distribution in the radial RF field, and completely different evolution trends of secular energy and total energy are observed in the cooling process. For the equilibrium ion system, the secular temperature can be reduced to a few milliKelvins, while the total temperature is considerably higher (2–3 orders of magnitude higher than the secular temperature). It appears that ion number does not restrict the realization of the milliKelvins magnitude of the secular temperature of the ion system. The micromotion characteristic is affected because of the space charge effect. When the 3D ion system reaches the equilibrium state, the micromotion energy of the outer ions is several orders of magnitude higher than that of the inner ions.

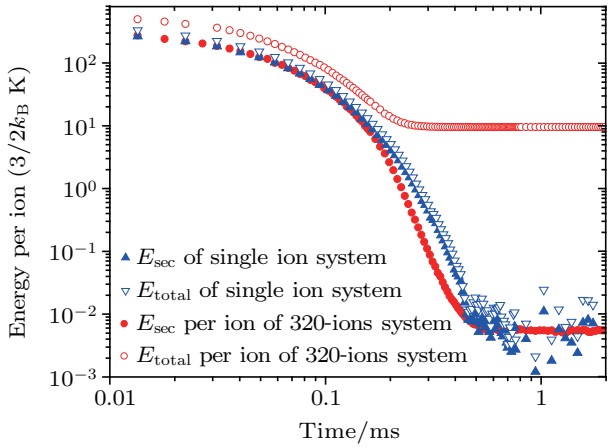


Fig. 2. (color online) Temporal evolutions of secular energy and total energy in laser-cooled single ion and 3D ion system under the same experimental parameters.

From Fig. 2, it can be observed that the secular temperature of the 3D ion system decreases more rapidly and the fluctuation in its secular temperature in the equilibrium state is smaller than that for the single ion. The reason for this is that the 3D ion system exhibits a random energy coupling effect between different ions on a 3D space scale, and the space charge effect of the ion system is helpful in increasing this effect and accelerating cooling to a certain extent. Moreover, the thermal energy in different dimensions is more easily removed by random photons during laser cooling. However, it is difficult for a single ion to realize 3D synchronous cooling because it exhibits a relatively small energy coupling effect. The equilibrium temperature of the 3D ion system is statistically averaged over the ion number, which reflects the overall energy characteristics of the ion system.

3.2. Influences of trapping potential on cooling efficiency and equilibrium temperature of ions

The 3D ion system achieves the radial confinement through dynamic RF potential and the axial confinement through the axial electrostatic potential in the linear Paul trap. Different radial and axial confinement strengths affect the space distribution and interaction characteristics of the ion system.[15,16] In addition, the cooling efficiency, equilibrium temperature, and other relevant characteristics of the ion system are influenced.

In a linear trap, trapping parameter q is related to the frequency and amplitude of the RF field and the structure characteristics of the ion trap.[17] Figure 3 shows the characteristics of cooling efficiency, ion temperature, and spatial configuration of the 3D ion system in the cooling process for different RF trapping potentials. Figures 3(a)–3(c) show the spatial distribution of the ion system (0.1 ms of delayed imaging) after cooling to the equilibrium state when $q = 0.14$, 0.3, and 0.45. The i and ii show the projective spatial distributions of the ion system in the radial (x–y) central plane and axial (y–z) central plane, respectively. As q increases, the radial confinement strength of ions increases gradually, their radial space distribution is compressed constantly, and the axial space distribution is extended continuously. When $q = 0.14$ and 0.3, the equilibrium ion system may maintain the crystal characteristics, where the track of micromotion in the direction $\boldsymbol{r}$ is relatively fixed and the behavior of secular motion around the axis center is confined to a respective lattice scale. However, when $q = 0.45$, the equilibrium temperature of the ion system increases, appearing in the liquid form, where the spatial distribution dispersion outline of the ion system is relatively fixed and the secular motion around the axis center is weakened to the position exchange of neighboring ions.

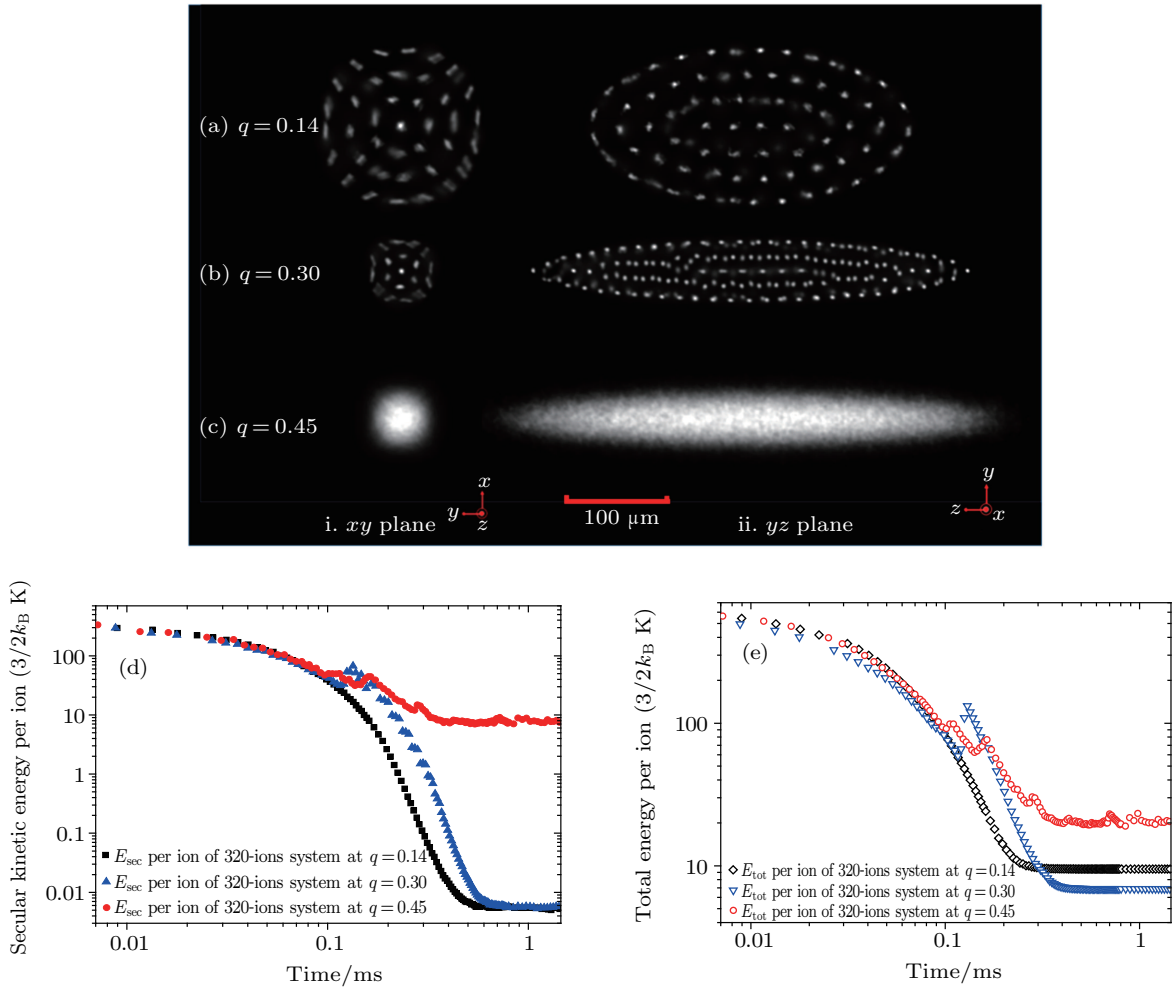


Fig. 3. (color online) Spatial distributions of the ion system (0.1 ms of delayed imaging) after cooling into the equilibrium state under different stable trapping parameters: (a) $q = 0.14$, (b) $q = 0.3$, and (c) $q = 0.45$. Temporal evolution characteristics of (d) secular energy and (e) total energy in the cooling process.

Figures 3(d) and 3(e) show the temporal evolutions of the secular and total energies of the ion system, respectively. The secular energy (Fig. 3(d)) and total energy (Fig. 3(e)) of the ion system can reach their respective values in equilibrium states at three trapping intensities. When q increases from 0.14 to 0.45, the cooling rates of the secular energy (Fig. 3(d)) of the ion system decrease. When $q = 0.14$ and 0.3, the secular temperatures of the ion system in the equilibrium state can reach

the same value. However, when $q = 0.45$, the secular temperature of the ion system in the equilibrium state increases. This shows that there is a critical trapping parameter, q_c, between the equilibrium energy characteristics and RF trapping strength of the ion system. When q is smaller than q_c, the energy coupling effect between the ion system and RF field is low, the ion system approximately satisfies the condition of quasi-adiabatic interaction, and the final temperature of ions primarily depends on the balance between the cooling effect and the random interaction heating effect. When q is higher than q_c, the coupling effect between the ion system and potential field is too large to be negligible, RF energy is coupled into the ion system to different extents, the ion system does not satisfy the condition of quasi-adiabatic interaction, the final temperature of ions depends on the balance among the cooling effect, RF heating effect, and random interaction, and the equilibrium temperature increases with trapping intensity increasing. As shown in Fig. 3(e), the total equilibrium energy of the ion system is the lowest when $q = 0.3$. This shows that selecting an appropriate RF trapping potential conduces to lowering the total equilibrium energy of ions and suppressing the ion micromotion effect and ion loss rate. However, it is necessary to prevent excessive RF trapping potential as it damages the quasi-adiabatic evolution characteristic of ions, which leads to the cooling failure of the ion system.

Figure 4 shows the influences of axial electrostatic trapping potential on the characteristics of cooling efficiency, equilibrium energy, and spatial configurations in the equilibrium state of the 3D ion system under constant experimental conditions. Figures 4(a) and 4(b) show the space distributions of the ion system (0.1 ms of delayed imaging) when it is cooled to the equilibrium state at $U_{end} = 3.500$ V and 10.500 V, respectively. The i and ii show the projections of the space distributions of the ion system in the radial (x–y) plane and the axial (y–z) central plane, respectively. As the axial electrostatic potential increases, the axial distribution is compressed constantly, the radial space distribution is extended continuously, and the equilibrium ion system always maintains crystal characteristics at low temperature. Figure 4(c) shows the temporal evolutions of the secular energy and total energy of the ion system in the cooling process at $U_{end} = 3.500$ V and 10.500 V, respectively. The secular energy and total energy of the ion system can reach the values in the equilibrium state eventually, and the evolution characteristics and equilibrium characteristics of the secular energy of the ion system do not change with the axial potential field. However, the space distribution of the ion system is extended in the radial direction as the axial potential field increases. The micromotion and total energies of the outer ions increase, and the total temperature of the ion system is high. Therefore, reducing the axial electrostatic potential as much as possible is conducive to suppressing the RF micromotion heating effect of the ion system and reducing the total energy of the ion system.

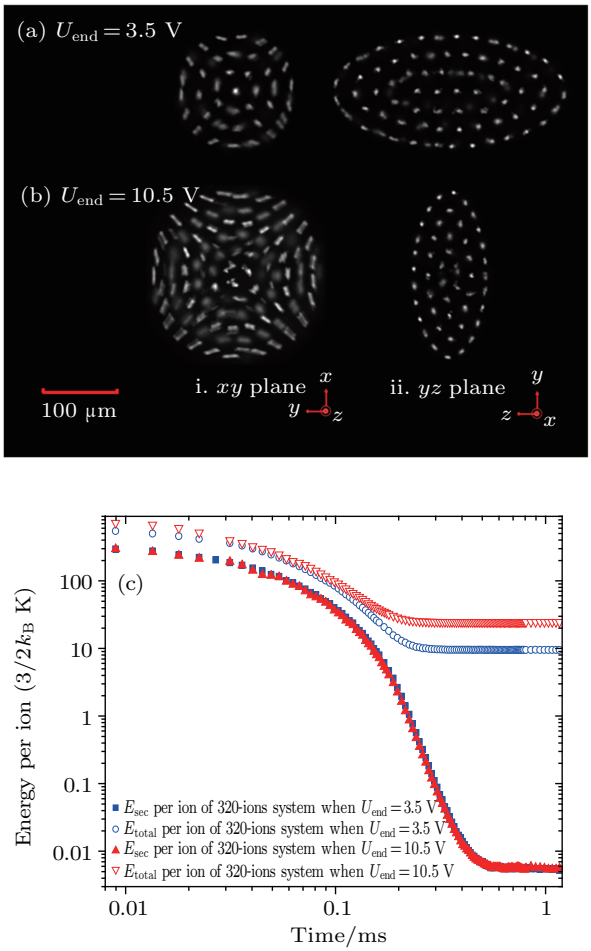


Fig. 4. (color online) Spatial distributions of the ion system (0.1 ms of delayed imaging) after cooling to equilibrium state under two axial electrostatic potentials: (a) $U_{end} = 3.500$ V and (b) 10.500 V. (c) Temporal evolution characteristics of secular energy and total energy in the cooling process.

3.3. Dynamic spatial distribution and temporal evolution of 3D ion system in cooling process

Because of the space charge effect, random photon recoil effect, etc., with the decrease of mean kinetic energy, the 3D ion system experiences a transformation among the different phases of gas, liquid, and solid (crystal) and eventually reaches the dynamic balance between cooling and heating.[18,19] In the cooling process, the motion models of all ions are coupled, and coupling strength depends on the temperature characteristic of the ion system. When ions are present in the cloud phase, their kinetic energy is considerably higher than the Coulomb interaction energy between ions and cooling efficiency is primarily determined by laser cooling force. With the decrease of the temperature of ions, when the kinetic energy of ions is comparable to the Coulomb interaction energy between ions, the ion system is in the liquid state. When the coupling strength of Coulomb force increases, the micromotion heating rate of ions increases and the cooling efficiency decreases gradually. When the kinetic energy of ions decreases to a value extremely

less than the Coulomb interaction energy between ions, the ion system lies in the range of strong Coulomb force coupling and the relative position between ions tends to be steady. In addition, the random interaction of Coulomb force is restrained gradually, and micromotion heating efficiency tends to be steady. Finally, the entire cooling efficiency tends to zero, in which case the ion system is in the equilibrium state.

Figure 5 shows the spatial distributions of 320 $^{40}Ca^{+}$ ions under different temperature conditions when the initial secular temperature is 400 K (delayed exposure time is approximately 1 secular motion period). The i and ii show the projections of the ion system in the (x–y) plane and the (y–z) central plane, respectively.

Figure 5(a) shows the transient spatial distribution (within a single secular motion period) when the secular temperature of the ion system is 239 K. The sizes of ions moving in the z and y directions are approximately 840.0 (26.4) μm and 480.0 (42.0) μm respectively, and each ion moves through the entire axial envelope of the ion system in the axial (z) direction. The motion distribution dispersion of the ion system is not clear in the radial cross section (x–y plane). The motion track is an overlap between rapid large-magnitude (radial) micromotion and slow large-magnitude (tangential) secular motion. The temporal evolution of the position vector of a specific ion can be dispersed in the entire 3D ion system envelope. The interaction between ions exhibits a global characteristic, the Coulomb force coupling is isotropic and lower in strength, and the ion system is characterized by the cloud state.

Figure 5(b) shows the transient spatial distribution (within a single secular motion period) when the secular temperature of the ion system decreases to 213 mK. The sizes of ions moving in the z and y direction are approximately 316.8 (4.2) μm and 168.0 (4.8) μm respectively, and the axial (z direction) motion of the ion presents frequent position exchange between neighboring ions. The spatial distribution dispersion outline of the ion system in the radial cross section (x–y plane) is relatively fixed. On one hand, the motion track is subjected to a relatively fixed radial micromotion track, and on the other hand, it is subjected to the relatively fixed secular motion behavior of tangential rotation position exchange. The temporal evolution of the position vector of a specific ion in the system is primarily distributed in a specific local space of the 3D system. The interaction between ions exhibits the local feature, the strength of Coulomb force coupling is improved, and the ion system is characterized by the liquid state.

Figure 5(c) shows the transient spatial distributions (within a single secular motion period) when the secular temperature of the ion system decreases to 1.7 mK. The sizes of the ions moving in the z and y direction are approximately 311.4 (1.2) μm and 153.0 (1.8) μm, respectively. It is impossible to observe the axial motion behavior of ions on a micrometer scale and a secular motion period time scale. The spatial distribution dispersion outline of the ion system in the radial cross section (x–y plane) is fixed, subjected to a certain radial micromotion track, and it is impossible to observe the secular motion behavior of the rotation position exchange of ions on a single secular motion period time scale. The temporal evolution of the position vector of a specific ion in the system is subjected to fixed local space coordinates. The strength of the Coulomb force coupling between ions is extremely high, the trends in coupling and motion are fixed and predictable, and the ion system is characterized by the crystal state.

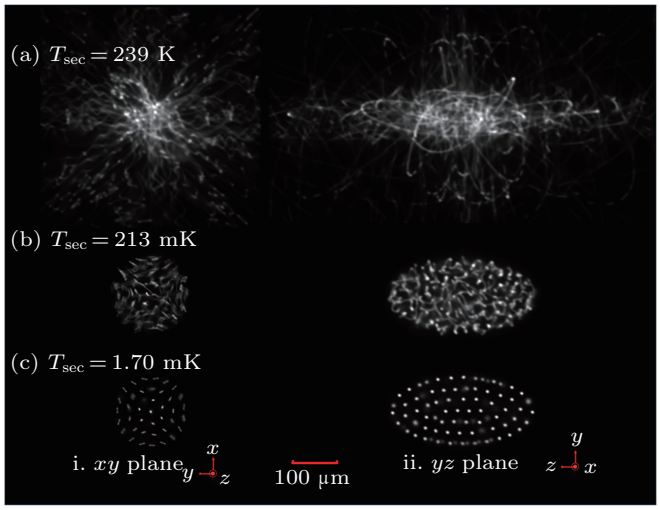


Fig. 5. (color online) Transient spatial distributions (exposure time is a single secular motion period) of laser-cooled 3D ion system at different temperatures.

The axial motion of the ion system in a linear Paul trap is less affected by RF micromotion modulation and primarily characterized by secular motion; it disperses into the entire ion system envelope at the high-temperature cloud state, and presents the frequent position exchanges between neighboring ions in the local space at low temperature liquid state; finally it is confined to a respective lattice scale at ultralow-temperature crystal state. The motion of the ion system in the radial plane is an overlap between secular motion and micromotion under RF modulation, which is manifested as micromotion with a relatively larger amplitude in the direction $\boldsymbol{r}$ and secular motion under fast rotation around the axis direction in the high-temperature cloud state. The amplitude of micromotion in the direction $\boldsymbol{r}$ decreases and the secular motion around the axial center is weakened to the position exchange of neighboring ions in the low-temperature liquid state. The micromotion track in the direction $\boldsymbol{r}$ is relatively fixed, and the behavior of secular motion around the axial center is confined to a respective lattice scale in the ultralow-temperature crystal state.

4. Conclusions and outlook

We propose a method of quantitatively evaluating the space charge effect of a 3D ion system and analyzing the space

charge effects on the cooling efficiency and the equilibrium temperature. The spatial distribution of an ion system on a secular motion period scale and the energy coupling feature in the cooling process are described. The results show that the space charge effect of the ion system is definitely correlated with the ion number, radial RF field, and axial electrostatic field. Among them, although the ion number is not a factor restraining the acquisition of the ion system at ultralow secular temperature, it affects the intrinsic micromotion feature of the ion system, and there exists an optimum matching relationship among the RF trap field, cooling efficiency, and equilibrium-state temperature of the ion system. Comparatively, the ideal cooling effect can be obtained when the stability trapping parameter $q \cong 0.3$. Axial electrostatic potential does not affect the evolution feature of the secular energy of ions, and on the premise of the stable trapping of the ions, the axial electrostatic potential decreasing as much as possible conduces to restraining the micromotion heating effect and the degradation of the total energy of the ion system. In a laser-cooled 3D ion system, the position vector of the ion will experience the process from the cloud state that disperses throughout the envelope of the ion system to the liquid state that concentrates in the specific local space of the ion system, and then to the crystal state, subjected to fixed motion track. This work is conducive to the studies of the spatial structure, phase transition, motional and dynamic properties, etc. in a 3D ion system, which plays an important role in realizing efficient cooling, lossless ion quantity, and quantum coherent manipulation of a 3D ion system, and in the improvement of the measurement precision of the ion spectra.

Acknowledgment

We would like to thank Shi Ting-Yun for our fruitful discussions.

References

[1] Vedel F and Andre J 1984 *Phys. Rev. A* **29** 2098
[2] Du L J, Song H F, Li H X, Chen S L, Chen T, Sun H Y, Huang Y, Tong X, Guan H and Gao K L 2015 *Chin. Phys. B* **24** 113703
[3] Wineland D J, Bollinger J J, Itano W M and Prestage J D 1985 *J Opt. Soc. Am. B* **2** 1721
[4] Todd J F J, Waldren R M, Freer D A and Turner R B 1980 *Int. J. Mass Spectrom. Ion Process.* **35** 107
[5] Roth B, Blythe P and Schiller S 2007 *Phys. Rev. A* **75** 023402
[6] Prestage J D, Williams A, Maleki L, Djomehri M J and Harabetian E 1991 *Phys. Rev. Lett.* **66** 2964
[7] Zhang C B, Offenberg D, Roth B, Wilson M A and Schiller S 2007 *Phys. Rev. A* **76** 012719
[8] Chen T, Du L J, Song H F, Liu P L, Huang Y, Tong X, Guan H and Gao K L 2014 *Chin. Phys. B* **23** 123702
[9] Berkeland D J, Miller J D, Bergquist J C, Itano W M and Wineland D J 1998 *J. Appl. Phys.* **83** 5025
[10] Du L J, Chen T, Song H F, Chen S L, LI H X, Huang Y, Tong X, Guan H and Gao K L 2015 *Chin. Phys. B* **24** 083702
[11] Verlet L 1967 *Phys. Rev.* **159** 98
[12] Verlet L 1968 *Phys. Rev.* **165** 201
[13] Zhang M Q and Skeel R D 1995 *J. Comput. Chem.* **16** 365
[14] Tolmachev A V, Udseth H R and Smith R D 2000 *Anal. Chem.* **72** 970
[15] Dehmelt H G 1969 *Adv. At. Mol. Phys.* **5** 109
[16] Berkeland D J, Miller J D, Bergquist J C, Itano W M and Wineland D J 1998 *J. Appl. Phys.* **83** 5025
[17] Paul W, Osberghaus O and Fischer E 1958 *Forschungsberichte des Wirtschafts und Verkehrsministeriums Nordrhein-Westfalen* **415** 1
[18] Slattery W L, Doolen G D and Dewitt H E 1980 *Phys. Rev. A* **21** 2087
[19] Mitchell T B, Bollinger J J, Dubin D H E, Huang X P, Itano W M and Baughman R H 1998 *Science* **282** 1290